nature communications

Article

https://doi.org/10.1038/s41467-025-63849-6

Scalable solution-processed ferroelectric polymers exhibiting markedly enhanced piezoelectricity

Received: 23 April 2025

Accepted: 27 August 2025

Published online: 01 October 2025

Check for updates

Ze Yuan[1,2], Hui Tong[3], Zekai Fei[1,2], Chenyi Li[1,2] & Yang Liu[1,2]

Intensive efforts have been made to enhance the weak piezoelectric coefficients of ferroelectric polymers for flexible and wearable devices. However, previous approaches are highly dependent on synthesis of desired composition and complex/hash processing conditions while the scalability remains rarely addressed limiting practical applicability. Here we report large piezoelectric coefficient d_{33} in scalable solution-processed ferroelectric poly(-vinylidene fluoride-*co*-trifluoroethylene) copolymers modified by C=C and C=O double bonds. We reveal that the introduction of C=C double bonds tune the energetic competition between ordered and disordered crystalline conformations. As a result, greatly enhanced d_{33} of −90.5 pC N^{-1} and dielectric constant of 22.7 are achieved, corresponding to about 3 times and 2 times as large as that of benchmark poly(vinylidene fluoride). We fabricate flexible and wearable sensors enabling detection of various signals such as pressure and sound with high sensitivity, which find promise in pressure mapping, health monitoring and acoustic sensing applications.

Lightweight and flexible ferroelectric polymers have been long commercialized from raw polymer powders, polymer products with varied shapes to various electronic and electromechanical devices used in civilian, medical, industrial and military areas[1–5]. However, the central obstacle limiting their piezoelectric applications hinges on the unsatisfactory piezoelectric coefficients[6]. For instance, piezoelectric coefficient d_{33} of the benchmark poly(vinylidene fluoride) (PVDF) remains as low as about −30 pC N^{-1} despite intensive studies during the past 5 decades[7–14]. To overcome this challenge, various approaches including morphotropic phase boundary (MPB)[15], high-field poling[16], and electrostriction[17] have been developed recently. A two-fold increase in d_{33} has been achieved[15,17–23] ($|d_{33}| > 60.0$ pC N^{-1}) since the observation of MPB in ferroelectric poly(vinylidene fluoride-*co*-trifluoroethylene) (P(VDF-TrFE)) copolymers[15]. Differing from initial efforts on achieving a high faction of polar all-*trans* conformation by stretching and poling[12,13], greatly enhanced near the MPB arises from the destabilization of the ordered all-*trans* into disordered 3/1-helix conformation[15]. Such *trans*/helix phase boundary generally occurs in ferroelectric polymers[15,17–19] whereas polarization rotation enabled by electric-field-induced phase transition from 3/1-helix to all-*trans* conformation is essential to enhanced d_{33} response[24,25]. In addition, an ultrahigh d_{33} of over 1000 pm V^{-1} is reported in P(VDF-TrFE-CFE) terpolymers (CFE: chlorofluoroethylene) modified by C=C double bonds under an electric field of 40 MV m^{-1} (ref. 26). This does not require noncentrosymmetric structure to intrinsically induce piezoelectricity while similar results have also been reported in inorganic piezoelectric oxides under a static electric field[27]. Moreover, large d_{33} obtained by these methods necessarily replies on the synthesis of commercially non-available polymer composition[15,23] such as P(VDF-TrFE) 50/50 mol% (ref. 15) and harsh/complex processing conditions such as ultrahigh cyclic poling field of 650 MV m^{-1} (ref. 16), a constant static field of 40 MV m^{-1} (ref. 26), a combination of hot-pressing, quenching, stretching, annealing and poling (ref. 17). The scalability, crucial to fabricate large rolls of piezoelectric films with a uniform thickness and d_{33}, has been rarely reported, presenting an obstacle for further industrial applications.

[1]State Key Laboratory of Material Processing and Die & Mould Technology, School of Materials Science and Engineering, Huazhong University of Science and Technology, Wuhan, Hubei, China. [2]Guangdong HUST Industrial Technology Research Institute, Guangdong Provincial Key Laboratory of Manufacturing Equipment Digitization, Dongguan, China. [3]Shanghai Acoustics Laboratory, Chinese Academy of Sciences, Shanghai, China. e-mail: yliu1319@hust.edu.cn

In this work, we report large intrinsic d_{33} in scalable P(VDF-TrFE) copolymers with C=C double bonds. We choose strongly alkaline NaOH to introduce C=C double bonds into P(VDF-TrFE) via the dehydrofluorination reaction[28–31], differing from previous works using alkalescent agents such as triethylamine mainly through dehydrochlorination reactions[26,32–38]. We find that C=C double bond defects can greatly modify the energetic landscape of P(VDF-TrFE) close to MPB, enabling stabilization of disordered 3/1-helix conformation against with ordered all-*trans* conformation. This offers an alternative tool to leverage the energetic competition between normal ferroelectricity and relaxor order which usually offers markedly enhanced properties. As a result, we observe that incorporation of a small amount of double bond defects of 0.86 mol% enables a sharp increase in $|d_{33}|$ from about 41.0 pC N^{-1} to 90.5 pC N^{-1} corresponding to over 40% enhancement over previous MPB approach[15,17–19]. The existence of large d_{33} is verified by both direct and converse piezoelectric measurements with the absence of a static electric field. Our scalable solution-processed films are characterized by a uniform d_{33}, a small variation in thickness, enhanced dielectric constant, increased elongation at break while piezoelectric sensors fabricated from these films show improved sensitivity. These findings unlock a new framework for massive manufacturing of next-generation high-performance ferroelectric polymers for promising flexible and wearable applications.

Results

Synthesis and characterization of P(VDF-TrFE) with C=C double bonds

In this work, P(VDF-TrFE) with the composition of 55/45 mol% close to its MPB regions[15,39,40] is chosen for double bond modifications. C=C double bonds are induced by dehydrofluorination reactions triggered by strongly alkaline NaOH[28–31] (Fig. 1a, top panel) differing from dehydrochlorination enabled by alkalescent agents revealed in Cl-contained polymers including P(VDF-CTFE), P(VDF-TrFE-CFE), P(VDF-TrFE-CTFE) (Fig. 1a, middle and bottom panels)[26,32–38]. Indeed, the reaction scheme (Fig. S1) in PVDF-based polymers has been studied in previous works[28–31]. The dehydrofluorination leads to the formation of unsaturated C=C double bond which may yield further crosslinking reactions leading to reduced C=C content[41]. Our results show that C=C double bond with a low NaOH concentration can be stable which is supported by complete dissolution into the solvent based on swelling experiments (Fig. S2). Above 0.9 mol%, crosslinking reactions are induced by the emergence of swelling effects inherent to the presence of crosslinking (Fig. S2). Such evolution arising from the reaction scheme is explicitly supported by Fourier-transform infrared (FTIR) spectroscopy. For instance, Fig. 1b shows that the presence of C=C double bond is confirmed by the characteristic infrared peak at around 1650 cm^{-1} (ref. 29). As NaOH dosage increases above 0.9 mol%, the characteristic peak density remains unchanged (Fig. 1b). This suggests that no additional C=C bonds forms due to the dehydrofluorination which in turn supports the formation of crosslinked structure. The saturation of C=C bonds occur near the critical NaOH content of about 0.9 mol%. Meanwhile, we find the presence of the infrared band at 1733 cm^{-1} corresponding to C=O double bonds[42], which is not revealed in the previous works[26,32–36]. The reaction scheme is summarized in Fig. S1. We show that the infrared band characteristic of C=O double bonds develops notably when NaOH dosage above 0.9 mol%, in constrast with that of C=C. Different from dual-functional C=C, C=O only behaves like defects which does not involve dehydrofluorination. The role of C=C and C=O in affecting d_{33} response will be analyzed later. Moreover, X-ray photoelectron spectroscopy (XPS) results show that C–H and C–F bond content decrease considerably with increasing NaOH dosage (Fig. 1c). This result indicates that dehydrofluorination still occurs which continues to produce unsaturated C=C bonds with the chararistic peak at around 285.0 eV (ref. 43). The excessive formation of unsaturated C=C double bonds may trigger the opening of C=C double bonds which generates C–C single bonds resulting in crosslinked chains. As mentioned above, the presence of crosslinked structure for NaOH dosage above 0.9 mol% is confirmed by swelling results (Fig. S2). ^{1}H nuclear magnetic resonance (NMR) was used to evaluate the C=C content (Figs. 1d and S3). The results show that C=C content is 0.86 mol% with a NaOH dosage of 0.9 mol% while it corresponds to 0.5 mol% with a NaOH dosage of 0.6 mol% (Fig. 1d). Consequently, these results elucidate the presence of C=C bonds at low NaOH dosage which saturates above 0.9 mol% accompanied by formation of crosslinked structure.

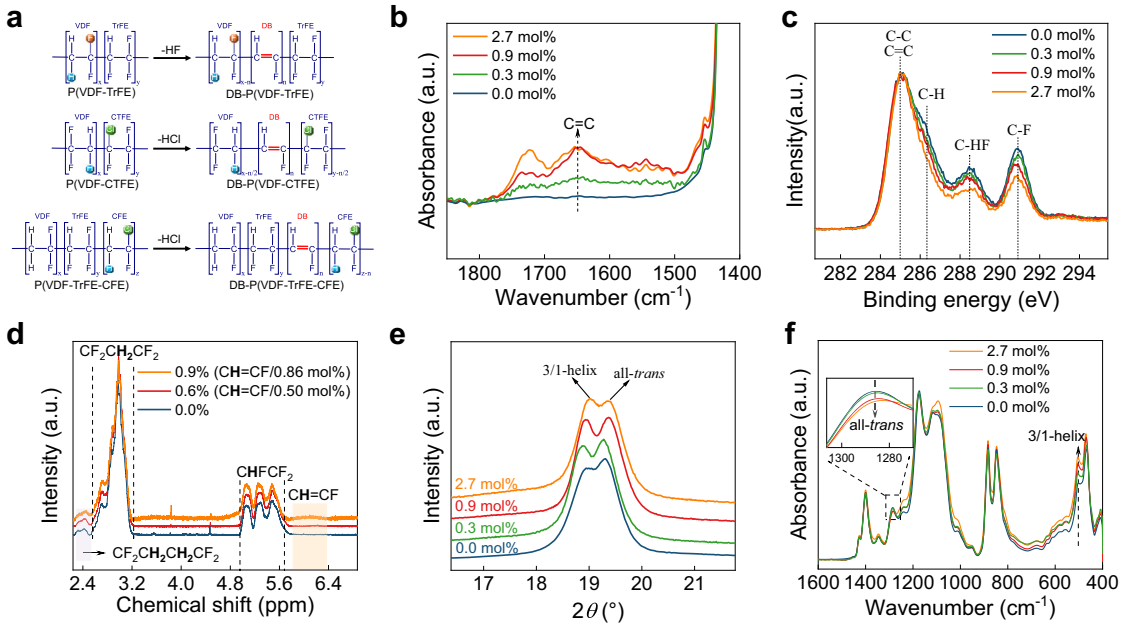

Fig. 1 | Structural characterization of double bond-modified P(VDF-TrFE). a The Scheme for the formation of C=C double bond in fluoropolymers. **b** FTIR spectra where the IR band characteristic of C=C is indicated at 1650 cm^{-1}. **c** C-spectrum XPS. **d** ^{1}H NMR spectra. **e** XRD patterns of double bond-modified P(VDF-TrFE), where the dashed arrows show the trend of all-*trans* and 3/1-helix changes with increasing NaOH dosage. **f** FTIR spectra of NaOH-modified P(VDF-TrFE), where the absorption peaks at 1285 cm^{-1} and 510 cm^{-1} corresponding to the all-*trans* and 3/1-helix conformation.

Structural characterization of P(VDF-TrFE) modified by various NaOH dosage is performed by XRD and FTIR. Pristine P(VDF-TrFE) is characterized by phase coexistence of all-*trans* and 3/1-helix conformations (Figs. 1e and S4) where the former remains the major phase (Figs. 1e and S5) according to the relative higher intensity for the peak at $2\theta = 19.3°$ (all-*trans*) than that at 18.9° characteristic of 3/1-helix[15,18,19]. Dehydrofluorination reaction not only induces the formation of C=C double bonds but also results in the decrease in VDF content. The latter may benefit the stabilization of 3/1-helix which is evident from the growth in the intensity for the peak assigned to 3/1-helix. Meanwhile, FTIR spectra provide further evidence to support the stabilization of 3/1-helix conformation and destabilization of all-*trans* conformation which can be seen by the notable development in the infrared band at 504 cm^{-1} and smearing of the infrared band at 1285 cm^{-1} (Fig. 1f). Consequently, recalling that tuning of the phase stability between all-*trans* and 3/1-helix conformations by varying the VDF content is essential to enhanced piezoelectric coefficients[15], the simultaneous realization of C=C double bonds and modifications of VDF content may offer an alternative way to tune the energetic landscape specifically for the pristine polymer composition close to MPB, benefiting d_{33} response.

Ferroelectric, dielectric and piezoelectric characterization

The existence of phase evolution enabled by including C=C double bonds is supported by polarization-electric field (*P-E*) hysteresis loops (Fig. S6). *P-E* loop is a key signature used to distinguish long-range and short-range ferroelectric orders. As pristine P(VDF-TrFE) is dominated by all-*trans* conformation (Fig. 2a), its *P-E* loop is typical ferroelectric with a remnant polarization P_r of 4.5 μC cm^{-2} and a coercive field E_c of 44.7 MV m^{-1} (Fig. 2b, c). Interestingly, P(VDF-TrFE) with C=C double bonds exhibit pinched type *P-E* loops (Fig. 2a) with a sharp drop in P_r and considerable decrease in E_c, reminiscent of those observed in relaxor ferroelectric polymers by changing polymer compositions[15,18,19]. The breaking of long-range ferroelectric instability induced by C=C double bonds is attributed to the stabilization of 3/1-helix conformation which is responsible for relaxor behavior in ferroelectric polymers[40]. Like compositionally-induced MPB, such destabilization of long-range ferroelectric distortion into short-range relaxor order is crucial to enhanced d_{33} response. This approach is completely different from initial studies on PVDF to achieve a high fraction of polar all-*trans* conformation with high polarization. Above the saturation point (0.9 mol%), E_c remains nearly unchanged with a continuous decrease in P_r resulting from crosslinking (Fig. 2b, c). These results indicate the dominant role of dehydrofluorination (Fig. S7) while defects such as polar C=O defects play a minor role. As the opening of C=C double bonds may trigger the formation of C–C single bond, therefore, enabling covalent bonding between adjacent polymer backbones. This yields a marked reduction in crystallinity leading to lowered remanent polarization as long-range ferroelectric instability mainly arises from crystalline regions of ferroelectric polymers. In addition, we find that

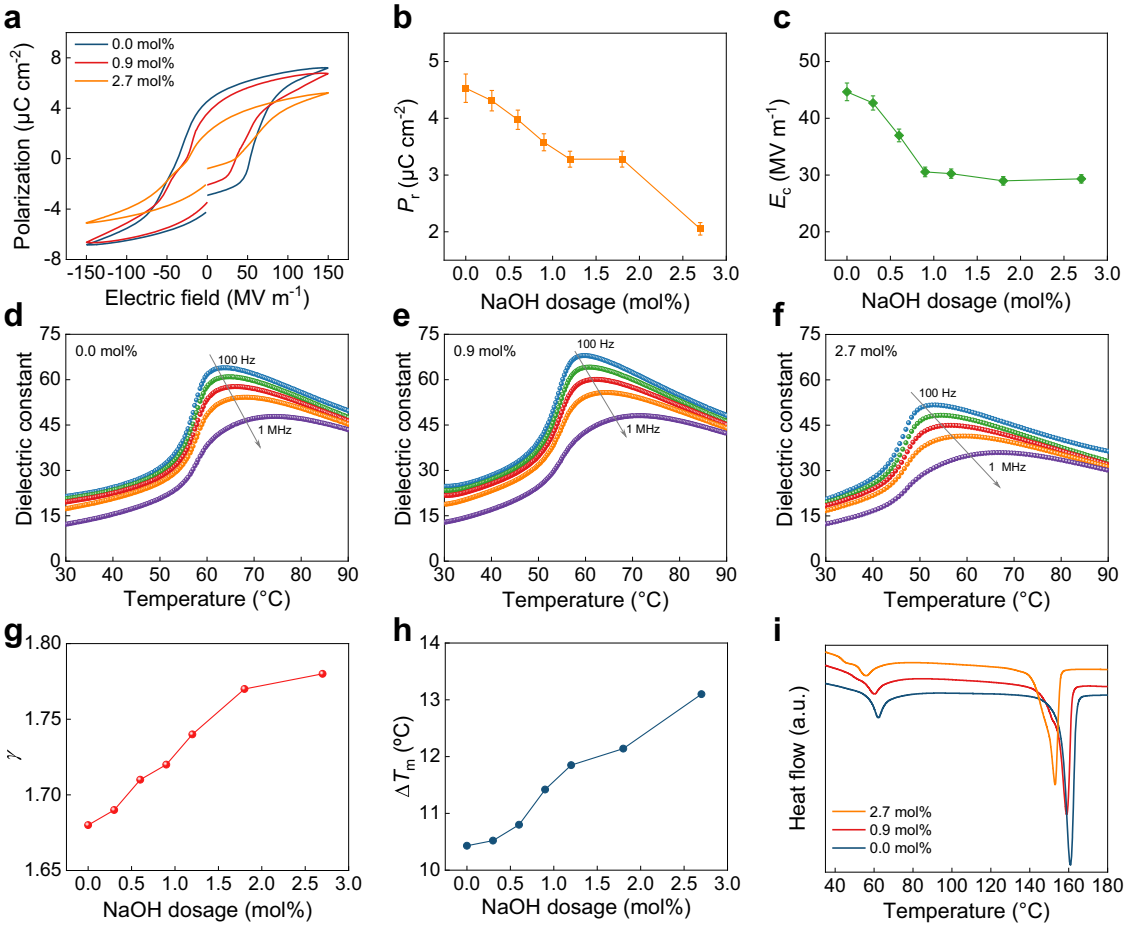

Fig. 2 | Ferroelectric, dielectric and thermal properties of double bond-modified P(VDF-TrFE). a *P-E* hysteresis loops. **b** P_r as a function of NaOH dosage. **c** E_c as a function of NaOH dosage. Dielectric constant versus temperature for various NaOH dosage **d** 0.0 mol%, **e** 0.9 mol% and **f** 2.7 mol%. The arrows in **d**–**f** denote the shift trend in T_m towards higher temperatures with the frequency increasing from 100 Hz to 1 MHz. **g** The relaxor diffuseness factor γ. **h** The ΔT_m defined as the frequency-dependent shift in T_m between 1 MHz and 100 Hz. **i** DSC heating scans. Error bars in **b** and **c** represent the standard deviation of the mean obtained from at least three measurements using different samples. Error bars in **b** and **c** represent standard deviations obtained from five measurements using different samples.

the inclusion of C=C and C=O defects induce a negligible change in leakage current behavior (Fig. S8) ruling out the presence of charged defects associated with the introduction of C=C and C=O defects. Consequently, *P-E* loop results demonstrate that incorporation of C=C defects stabilize disordered helix conformation through breaking the long-range ferroelectric distortion, which is well consistent with structural results.

Dielectric spectra under different frequencies upon heating is used to evaluate the evolution in short-range ferroelectric order (Figs. 2d–f and S9-S11). The pristine composition P(VDF-TrFE) 55/45 mol% displays the coexisiting ferroelectric and relaxor phases with the relaxor phase as a minor phase (Figs. 1e, 2a and 2d). The emergence of relaxor behavior is characterized by a strong shift in the dielectric peak temperature T_m towards higher temperatures as the frequency increases (Fig. 2d). In modified P(VDF-TrFE), it is found that relaxor behavior becomes stronger in terms of a broader dielectric peak at a specific frequency and marked decrease in the dielectric peak value (Fig. 2e, f). The broad dielectric peak is fitted by modified Cuire–Weiss relationship, which yields a diffuseness factor γ indicative of strength of relaxor phase (Fig. S12). It is found that γ increases as NaOH content increases, supporting the growth of relaxor phase (Fig. 2g). In addition, the temperature difference ΔT_m between T_m at 100 Hz and 1 MHz experiences a considerable increase (Fig. 2h), collaborating with stronger relaxor characteristics. In addition, the endothermic peak at around T_m is smeared in differential scanning calorimetry (DSC) heating scans (Figs. 2i and S13-S19), supporting more diffused phase transition due to the inclusion of C=C double bonds. Consequently, these results further support the stabilization of 3/1-helix conformation induced by incorporating C=C double bonds which is characterized by the growth of relaxor behavior.

Structural and electrical results indicate that the energetically more favorable phase evolves from ordered all-*trans* to disordered helix enabled by the inclusion of C=C double bonds instead of decreasing VDF content in previous compositional approach[15,39]. Moreover, the presence of C=C and C=O double bonds may provide additional contribution to the piezoelectric response offering opportunities to compete favorably with previous compositional approach[15]. In this regard, piezoelectric measurements are performed on pristine and modified P(VDF-TrFE) by using d_{33} meter and electric field-induced strain (Figs. 3a, b and S20a). To verify our measurement results, we focus on d_{33} of pristine P(VDF-TrFE) 55/45 mol% copolymer which has been measured in previous works. Our results show a d_{33} of −41.0 pC N^{-1} and −40.0 pm V^{-1} (Figs. 3a, b and S20a), respectively, which is well consistent with previous results[15,44]. Meanwhile, through our piezoelectric measurements, d_{33} of commercial PVDF is −26.0 pC N^{-1} (Fig. S21) and −26.4 pm V^{-1} (Fig. S22), respectively, which also agree with recent results[7–14]. The good agreement between different measurement techniques on different polymer compositions strongly substantiates the piezoelectric results obtained by other synthesized polymers. Interestingly, it is found that as NaOH dosage increases, d_{33} exhibits an abrupt increase reaching the maximum of −90.5 pC N^{-1} at a critical NaOH dosage of 0.9 mol% (or 0.86 mol% C=C double bond), which is followed by dramatic drop in the crosslinking region (Fig. 3a, Fig. S20b, Movie S1). The electric field-induced strain manifesting the converse piezoelectric effect yields a converse piezoelectric coefficient d_{33} of −91.8 pm V^{-1} (Fig. 3b), which verifies the existence of substantially enhanced piezoelectric response induced by C=C double bonds (Fig. S7). This corresponds to 3 times as large as that of PVDF[7–14], which also outperforms other results[15,17–22] in P(VDF-TrFE) (see Table S1). We note that crystallinity decreases slightly from 55% to 51% when NaOH dosage increases from 0 mol% to 0.9 mol% (Fig. S25). This result indicates a minor role in decreasing d_{33} response caused by reduced crystallinity. The markedly lowered crystallinity induced crosslinking for NaOH dosage above 0.9 mol% implies that the reduction in the enhancement in d_{33} may result from the reduced crystallinity. Consequently, these results confirm the existence of markedly enhanced d_{33} enabled by incorporating C=C defects.

In addition to d_{33} (Fig. 3d), piezoelectric voltage constant g_{33} and figure of merit $d_{33}\times g_{33}$ -key parameters to evaluate the suitability of piezoelectric materials for energy harvesting and sensing applications- are also compared. We show that g_{33} and $d_{33}\times g_{33}$ are markedly improved in modified polymers (Fig. 3e, f and Table S2). The

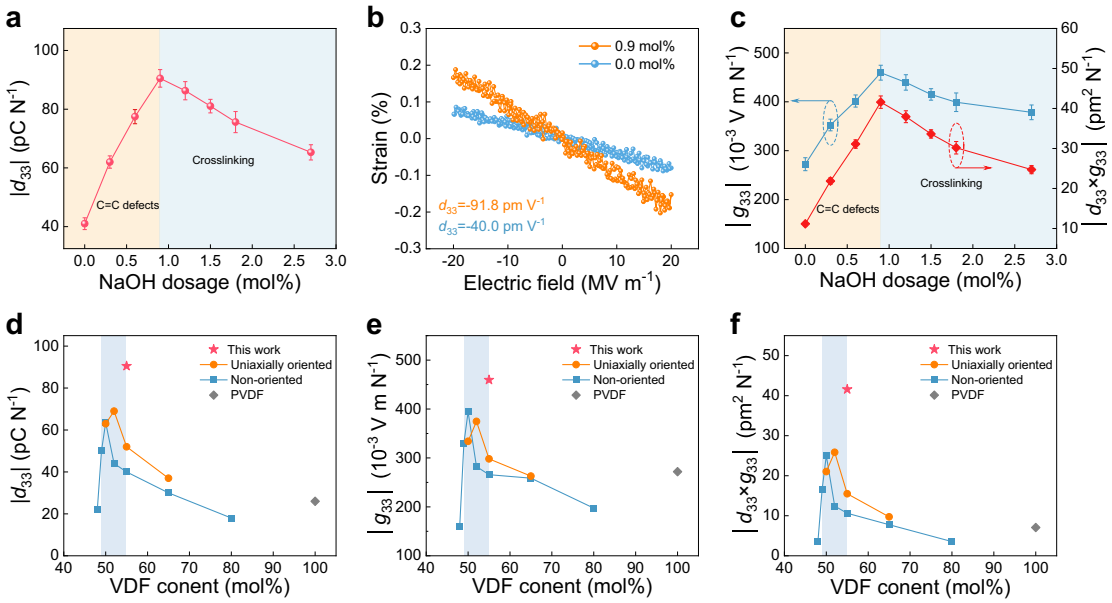

Fig. 3 | Enhanced piezoelectric properties induced C=C double bond. a The d_{33} results measured using d_{33} meter. (The error range is based on 30 independent samples.) **b** Strain induced by an electric field at 1 Hz whereas the slope is indicative of d_{33} via the converse piezoelectric effect. **c** g_{33} and $d_{33}\times g_{33}$ as function of NaOH dosage. (The error range is based on 30 independent samples.) **d** Comparison of d_{33}. **e** Comparison of g_{33}. **f** Comparison of $d_{33}\times g_{33}$. Non-oriented data were taken from ref. 15 and uniaxially oriented data were taken from ref. 17. Error bars in **a** and **c** represent the standard deviation of the mean obtained from at least three measurements using different samples. Error bars in **a** and **c** represent standard deviations obtained from five measurements using different samples.

highest $|g_{33}|$ of 459.5 × 10^{-3} V m N^{-1} is achieved for the NaOH dosage of 0.9 mol% (Fig. 3c), which exceeds that (394.1 × 10^{-3} V m N^{-1}) obtained by compositionally driven MPB (P(VDF-TrFE) 50/50 mol%). Meanwhile, the figure of merit is 41.6 pm^2 N^{-1} in modified P(VDF-TrFE) surpasses that (25.0 pm^2 N^{-1}) of P(VDF-TrFE) with MPB composition (Table S2). These results suggest the promise of double-bond modified copolymers in developing high-performance energy harvesters and sensors.

The enhanced piezoelectric response is achieved without the requirement of a static electric field, differing from that obtained in previous work[26]. Given that the formation of C=C double bonds also involve the compositional change in VDF content through the dehydrofluorination, it is estimated that C=C and C=O double bonds themselves might account for over 40% of total enhancement in d_{33} based on the comparison between the results obtained in this work and that achieved by compositionally-induced MPB[15]. The more electroactive ability induced by including C=C and C=O double bonds is evident from the large increase in dielectric constant (Figs. S23 and S24). In addition, only a slight decrease in crystallinity is found by incorporating a small amount of C=C double bonds (Fig. S25), which suggests a minor role of amorphous phase in affecting d_{33} response. The presence of C=C double bonds may ease the local polarization rotation in the crystalline phase, leading to the enhanced d_{33}. Further theoretical studies are highly desired to reveal the crucial role of C=C double bond in improving d_{33} response[45]. Moreover, it is found that the benefit of enhancement in d_{33} enabled by C=C double bond requires polymer composition with a flattened energetic landscape i.e., close to MPB. For instance, it is shown that the absence of markedly enhanced piezoelectric response is observed for P(VDF-TrFE) with a well-defined ground state (i.e., VDF = 80 mol%, Fig. S26), which indicates the importance of nearly energetically degenerate phases in generating large piezoelectric response. Further studies are highly desired to modify the energetic landscape near MPB of ferroelectric polymers by using various chemical defects which generally involve a rich source of polymers such as terpolymers and polymer blends. Consequently, these results indicate the promise of chemical defects[46] in optimizing intrinsic functionalities of ferroelectric polymers which should be generally applicable to other polymer compositions and other properties.

Scalability

Given that high d_{33} exceeding commercial PVDF has been achieved by various approaches, the scaling potential has not been addressed, limiting large-scale practical applications. For instance, ultrahigh poling field of 650 MV m^{-1} close to the breakdown field can be only used to pole small-size sample[16] which may cause breakdown failure of polymer films for large scale applications. To explore the scaling potential, we fabricate solution-processed freestanding films with a size identical to A4 paper (Fig. 4a). The process of modified ferroelectric polymers does not require mechanical stretching as required in PVDF whereas flat film surface is challenging for orientation process[10] (Fig. 4b). By contrast, solution-processed films show a much flatter surface (Fig. 4c) than PVDF (Fig. 4b) fabricated by extrusion-orientation and hot-pressing technique[47]. Meanwhile, PVDF film thickness by orientation process typically exceeds 10 μm while our solution-processed films do not show such limitation in thickness scaling, which is of importance for device miniaturization and integration. We also examine the thickness dependance on d_{33} as scalability. The results show that d_{33} is independent of film thickness (Fig. S27) further indicating the presence of intrinsically large piezoelectric properties in modified P(VDF-TrFE), which is like commercial stretched PVDF. We find that a uniform d_{33} response is confirmed in flexible films (Fig. 4d) with a small variation in the film thickness (Fig. 4e), indicating the good scalability. Moreover, the dielectric constant exceeds that of PVDF by about 90% (Figs. 4f and S23 and S28a), which also benefits device miniaturization and integration owing to increased capacitance. The dielectric constant of PVDF and modified P(VDF-TrFE) generally decreases as the frequency of the external electric field increases (Fig. 4f). This is because orientational polarization cannot keep up with the rapid variation in the applied electric field at high frequencies. We show that dielectric loss of modified P(VDF-TrFE) remains nearly the same as that of PVDF at 1 kHz (Fig. S28b). Meanwhile, for durability of the vibrational device, it requires piezoelectric polymers with high elongation

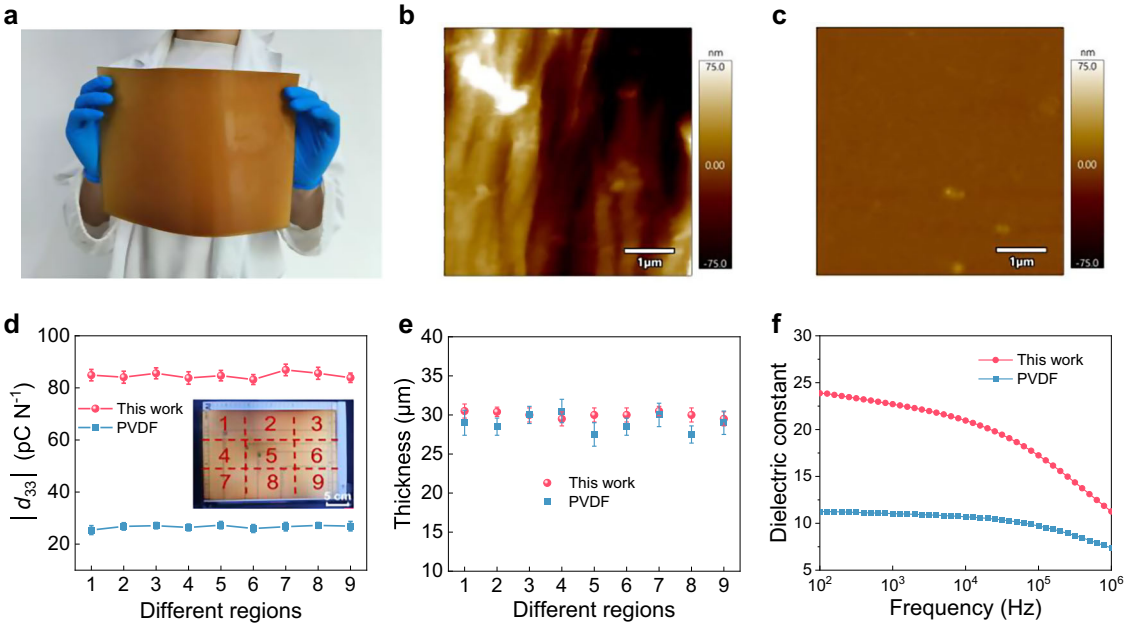

Fig. 4 | Scalability. a Photo of solution-processed films. **b** Atomic force microscopy (AFM) topography of commercial PVDF films. **c** AFM topography of solution-processed films. **d** The d_{33} uniformity test with a film size identical to A4 paper where the inset shows double bond -modified P(VDF-TrFE) films and different regions. **e** Thickness uniformity result. **f** Comparison of dielectric constant between PVDF and modified P(VDF-TrFE) films. Error bars in **d** and **e** represent the standard deviation of the mean obtained from at least three measurements using different samples. Error bars in **d** and **e** represent standard deviations obtained from five measurements at selection regions.

at break. We find that our modified films exhibit improved elongation at break up to 210% (Fig. S29), outperforming that of PVDF. Consequently, these results offer a new avenue for reconciling large piezoelectric properties and scalability to enable integration into massive manufacturing of next-generation ferroelectric polymers for flexible and wearable applications.

Piezoelectric energy harvesting and sensing applications

Although C=C double bonds have been previously used to yield a giant converse piezoelectric d_{33} (ref. 26), it requires applying a static electric field which is not suitable for practical devices enabling the conversion of mechanical energy to electrical energy such as pressure and sound sensors. In this regard, to demonstrate the promise in flexible and wearable devices using C=C double bond modified P(VDF-TrFE), we fabricate pressure sensors (Figs. S30 and S31). We show that the open-circuit voltage measured under different stresses (Figs. 5a, S32 and S33) describes good linear dependence, in agreement with piezoelectric nature. This result is different from the nonlinear response with increasing the pressure obtained in a recent work[45] which reported a large d_{33} of −191.4 pC N^{-1}. Through the slope of voltage-pressure curve, pressure sensitivity can be obtained. Commercial stretched PVDF is known to show good energy harvesting properties and its pressure sensitivity is 8.11 mV kPa^{-1} (Figs. 5b and S33) which agrees with previous results[48,49]. We show that the pressure sensitivity (Fig. 5b) of pristine P(VDF-TrFE) is about 7.55 mV kPa^{-1}, which is consistent with previous sensor performance (i.e., 4.56 mV kPa^{-1} in ref. 50 and 6.10 mV kPa^{-1} in ref. 51) based on P(VDF-TrFE) copolymers. Moreover, via double bond modifications, we find that the deduced pressure sensitivity is improved up to 14.22 mV kPa^{-1} much larger than both stretched PVDF and pristine P(VDF-TrFE), which mainly originates from greatly enhanced d_{33}. We show that the capacitance before and after device fabrication remains slightly reduced (Fig. S34). Meanwhile, we find that the induced voltage displays almost no degradation up to 10^5 mechanical cycles (Fig. S35), demonstrating excellent durability upon vibrational testing. In addition, we find that senor performance remains unchanged under varied temperature (Fig. S36), humidity (Fig. S37) and mechanical strength (Fig. S38), suggesting excellent device stability. We also show that our device can detect small pressure above 8 kPa (Fig. S39), which is mainly limited by the force generator in our experimental setup. Based on the pressure sensitivity results (Fig. S39), we estimate that weak signals as low as tens of Pa can be resolved by our sensor based on modified polymers (Fig. S40).

The induced voltage and pressure sensitivity are strongly dependent on intrinsic factors (such as d_{33}, dielectric constant, the Young's modulus) and extrinsic factors (i.e., film thickness, encapsulation conditions, measurement conditions among different devices)[51–53]. For instance, regarding the intrinsic factors, although d_{33} of modified polymers is about 2.26 times as large as that of pristine counterparts, dielectric constant is also enhanced by 33% which tends to decrease the induced piezoelectric voltage. By assuming the same modulus, thickness and extrinsic conditions, the voltage generated by modified polymers is about 1.7 times as big as that of pristine counterparts which is in line with the observed experimental results.

We further show that these flexible sensors are ideal for wearable applications. For instance, we show that a wrist-worn sensor device made of modified P(VDF-TrFE) film (Fig. 5d) can distinguish the pulse wave signals at rest and after exercise (Fig. 5e). The observed physiological differences show the high sensitivity to weak signals, suggesting broad application prospects in wearable health monitoring systems. We also attach the sensor to the throat to record the signal waveforms of different spoken words (Fig. 5f). The results clearly distinguish different pronunciations (Fig. 5g, Movie S2 and S3), which indicates the potential application in acoustic sensing and speech recognition technology.

Discussion

C=C double bonds have been regarded as the important defects in driving enhanced electrocaloric and electrostrictive effects in ferroelectric polymers[26,32–34]. The role of C=C defects in driving the phase transition through the dehydrofluorination reactions (Fig. S7) has not been revealed in previous studies[26,32–36]. Meanwhile, near the MPB in irradiated ferroelectric polymers, whereas the irradiation-induced oxidation reactions also introduce C=O defects[5,24], an enhanced d_{33} of −70 pC N^{-1} is observed exceeding that (−63.5 pC N^{-1}) obtained by

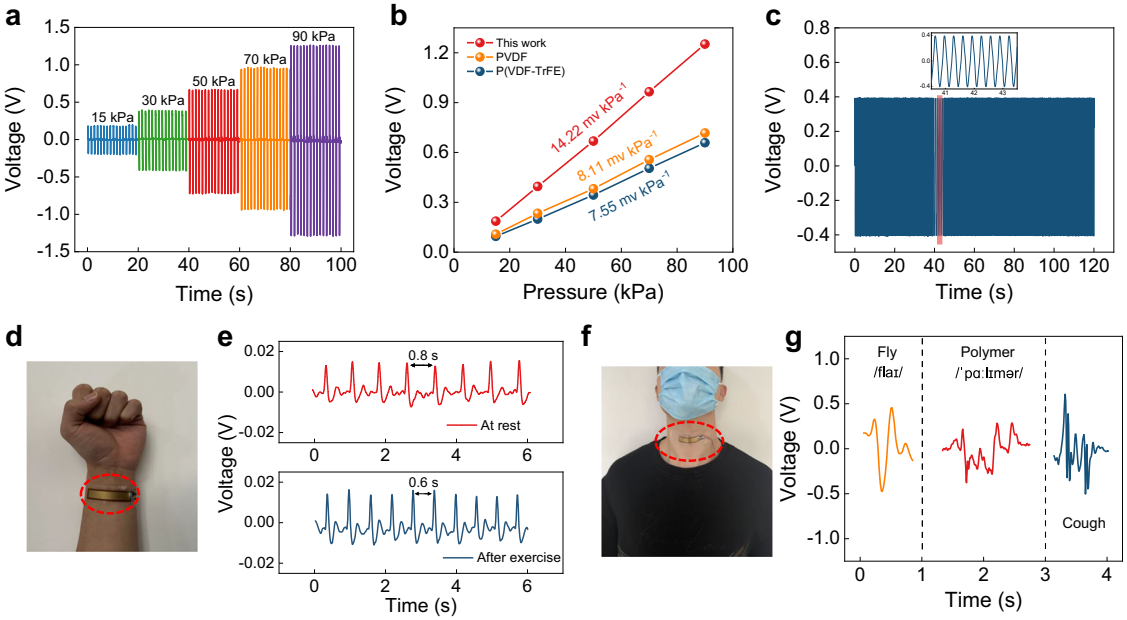

Fig. 5 | Energy harvesting and piezo-sensor devices using double bond-modified P(VDF-TrFE). a Open-circuit voltage of double bond-modified P(VDF-TrFE) with different stresses at 3 Hz. **b** Pressure sensitivity of PVDF, pristine P(VDF-TrFE) and double bond-modified P(VDF-TrFE) at 3 Hz. **c** Piezoelectric response stability test after 10^4 cycles under 30 kPa at 3 Hz. **d** Photo of a wrist-mounted sensor. **e** Pulse wave signal measurement at resting and after exercise. **f** Photo of sensor device attached to the throat. **g** Signal waveforms of different word pronunciations.

compositionally induced MPB[24]. The polarization rotation mechnism[25] is crucial to enhanced d_{33} in previous works[15,24].

In our case, we provide further analysis of the relative contribution of C=C and C=O to the enhanced d_{33}. For NaOH dosage above 0.9 mol% (i.e., 2.7 mol%), the development of C=O double bonds is evident from the notable expansion of infrared bands in FTIR results (Fig. 1b). However, a dramatical decline in d_{33} is observed in this regime (>0.9 mol%) suggesting a minor role of increased C=O double bonds in improving d_{33} response. Instead, dual functional C=C is mainly responsible for large d_{33} in modified P(VDF-TrFE). To further support this scenario, we focus on the optimal compositions under varied reaction time (Fig. S41). We show that as the reaction time increases, the content of C=O is almost saturated under a short reaction time 0.5 h while the content of C=C reaches the maximum at a reaction time of 2 h (Fig. S41a and S41b). Meanwhile, $|d_{33}|$ exhibits a notable increase when the reaction time is from 0.5 h to 2 h. For the reaction time above 4 h, we observe considerably reduced C=C content which is accompanied by a decrease in $|d_{33}|$ (Fig. S41c). This result, therefore, suggests the dominant role of C=C double bonds in determining the enhancement in d_{33} response.

Methods

Synthesis of P(VDF-TrFE) with C=C double bond

The 5 g of P(VDF-TrFE) copolymer (Piezotech at Arkema, the composition ratio of VDF/TrFE=55/45 mol% and 80/20 mol%) was dissolved in 50 mL of N,N-dimethylformamide (DMF, Sigma-Aldrich) and the polymer solution was stirred at room temperature for 12 h. Subsequently, NaOH with varied dosage was added to polymer solution under the N_2 atmosphere and the dehydrofluorination reaction was controlled by varying the amount of NaOH (x mol% of NaOH with respect to P(VDF-TrFE) was added). The reactions were done under the same N_2 atmosphere to fix the same reaction conditions. For instance, this can effectively avoid direct reactions with O_2 in the air. The reaction condition was conducted at room temperature with stirring at 600 rpm for 2 h. The mixture solution was centrifuged to remove the precipitated byproducts. The centrifuged solution was cast onto the glass substrate and dried in a vacuum oven at 80 °C for 12 h. Then, the sample was annealed in a vacuum oven at 140 °C for 12 h. The typical film thickness was 40 μm. Stretched PVDF with varied thickness was purchased from PolyK Technologies.

XRD

The crystal structure was determined using XRD on an Empyrean diffractometer (PANalytical) with Cu-Kα radiation, with a 2θ scan from 15° to 25° at a step of 0.02°.

FTIR

FTIR spectroscopy was performed using a Nicolet iS50R spectrometer (Thermo Scientific) with a wavenumber range of 4000–400 cm^{-1}.

DSC

Thermal properties were analyzed by DSC using a Diamond DSC (PerkinElmer) under N_2 atmosphere. The heating scans were from 30 °C to 200 °C at a heating rate of 10 °C min^{-1}. Crystallinity (X_c) was calculated from the melting enthalpy (ΔH_m) using the equation: $X_c = \Delta H_m/[x_{VDF}\Delta H_0]$, where $\Delta H_0 = 103.4$ J g^{-1} and x_{VDF} was the VDF molar fraction.

Swelling test

Sample of 20 mg with varied NaOH dosage was dissolved in 20 mL of DMF at room temperature for 48 h.

NMR

The degree of dehydrofluorination (double bond content) was quantified by ^{1}H NMR spectroscopy using an AscendTM 600 MHz spectrometer (Bruker). The double bond content was determined by $A_4/(A_1 + 0.5A_2 + A_3 + A_4)$, where A_i is the area of characteristic peak: A_1(2.2 ppm–2.5 ppm), A_2 (2.5 ppm–3.2 ppm), A_3 (4.8 ppm–5.8 ppm) and A_4 (5.8 ppm–6.4 ppm).

XPS

Carbon 1s (C1s) binding energy was analyzed by XPS using a SCIENTIFIC ESCALAB 250Xi spectrometer (Thermo Scientific).

AFM

The surface topography of the sample was characterized using AFM. The measurement instrument was Jupiter XR (Oxford Instruments Asylum Research). The probe used in the experiment was SNL 10 (Bruker) with the nominal spring constant of 0.35 N m^{-1}.

Dielectric testing

Dielectric constant under different temperatures and frequencies (frequency range: from 100 Hz to 1 MHz; temperature range: from 10 °C to 100 °C) was measured using an LCR meter (E4980A, Keysight) and an impedance analyzer (Agilent 4294A), with a heating rate of 1 °C min^{-1}. The dielectric constant above T_m (1 MHz) was fitted by using modified Curie–Weiss relation expressed as $(T\text{-}T_m)^\gamma/C = 1/\varepsilon_r\text{-}1/\varepsilon_{max}(T = T_m)$ (γ is the relaxor diffuseness factor, C is a constant and $\varepsilon_{max}(T = T_m)$ is the dielectric peak value).

Ferroelectric testing

P-E loops were recorded using a modified Sawyer-Tower circuit whereas an electric field with a triangular bipolar wave and 10 Hz was used.

Corona poling

A home designed setup was used to enable poling of polymer films with a voltage of 15 kV and tip-film distance of about 4 cm. The charging time was 10 min.

Piezoelectric measurement

Piezoelectric coefficient d_{33} was evaluated using a PKD3-2000 tester (PolyK Technologies) via the quasi-static Berlincourt method (static force: about 0.5 N, dynamic force: 0.25 N, measurement frequency: 110 Hz). The converse d_{33} was measured with a laser interferometer (SIOS SP-S 120E) with a frequency of 1 Hz. Before piezoelectric measurements, polymer films were polarized by contact poling (10 min at a DC electric field of 150 MV m^{-1}) and the size of samples was typically 1 cm × 1 cm.

Sensor device preparation

The sketch of device fabrication was summarized in Fig. S31. The gold layer, ~500 nm in thickness, was deposited onto the sample surface via magnetron sputtering to function as electrodes (Quorum Q150RS plus). Subsequently, the sample was encapsulated with polydimethylsiloxane (PDMS). The electrodes on both sides were connected to copper wires using pressure terminals for the transfer of charge generated by strain. Then, a flexible wearable piezoelectric sensor device was fabricated for subsequent performance evaluation. All samples underwent corona polarization before the PDMS encapsulation.

Characterization of sensor device

A pressure-controlled motor (PR-BDM8-100F, PURI Materials) was utilized to apply pressures ranging from 10 to 200 kPa to the sample at room temperature. The output signal from the sensor was amplified using a low-noise current preamplifier (SR570, Stanford Research Systems) and the resulting voltage was recorded with a digital oscilloscope (InfiniiVision MSO-X3054A, Keysight) featuring an input impedance of 1 MΩ. The authors have a signed informed content from

the research participates depicted in Fig. 5 and declare an ethics approval has been waived by the ethics committee.

Data availability

The source data for Figs. 1–5 in this work are provided in the Source Data file. Source data are provided with this paper. All data are available from the corresponding author upon request.

References

1. Lovinger, A. J. Ferroelectric polymers. *Science* **220**, 1115–1121 (1983).
2. Ribeiro, C. et al. Electroactive poly(vinylidene fluoride)-based structures for advanced applications. *Nat. Protoc.* **13**, 681–704 (2018).
3. Liu, Y. & Wang, Q. Ferroelectric polymers exhibiting negative longitudinal piezoelectric coefficient: progress and prospects. *Adv. Sci.* **7**, 1902468 (2020).
4. Liu, Y. et al. Electro-thermal actuation in percolative ferroelectric polymer nanocomposites. *Nat. Mater.* **22**, 873–879 (2023).
5. Li, C. Y. et al. Enhanced energy storage in high-entropy ferroelectric polymers. *Nat. Mater.* **24**, 1066–1073 (2025).
6. Ramadan, K. S., Sameoto, D. & Evoy, S. A review of piezoelectric polymers as functional materials for electromechanical transducers. *Smart Mater. Struct.* **23**, 033001 (2014).
7. Furukawa, T. & Seo, N. Electrostriction as the origin of piezoelectricity in ferroelectric polymers. *Jpn. J. Appl. Phys.* **29**, 675 (1990).
8. Bystrov, V. S. et al. Molecular modeling of the piezoelectric effect in the ferroelectric polymer poly(vinylidene fluoride) (PVDF). *J. Mol. Model.* **19**, 3591–3602 (2013).
9. Darestani, M. T. et al. Piezoelectric membranes for separation processes: Fabrication and piezoelectric properties. *J. Membr. Sci.* **434**, 184 (2013).
10. Sencadas, V., Gregorio, R. Jr. & Lanceros-Méndez, S. α to β phase transformation and microestructural changes of PVDF films induced by uniaxial stretch. *J. Macromol. Sci.* **48**, 514–525 (2009).
11. Katsouras, I. et al. The negative piezoelectric effect of the ferroelectric polymer poly(vinylidene fluoride). *Nat. Mater.* **15**, 78–84 (2016).
12. Kepler, R. & Anderson, R. Piezoelectricity and pyroelectricity in polyvinylidene fluoride. *J. Appl. Phys.* **49**, 4490–4494 (1978).
13. Gomes, J., Serrado Nunes, J., Sencadas, V. & Lanceros-Mendez, S. Influence of the β-phase content and degree of crystallinity on the piezo- and ferroelectric properties of poly(vinylidene fluoride). *Smart Mater. Struct.* **19**, 065010 (2010).
14. Jaglan, N. & Uniyal, P. On the structural, dielectric, piezoelectric, and energy storage behavior of polyvinylidene fluoride (PVDF) thick film: Role of annealing temperature. *J. Appl. Phys.* **132**, 224109 (2022).
15. Liu, Y. et al. Ferroelectric polymers exhibiting behaviour reminiscent of a morphotropic phase boundary. *Nature* **562**, 96–100 (2018).
16. Huang, Y. et al. Enhanced piezoelectricity from highly polarizable oriented amorphous fractions in biaxially oriented poly(vinylidene fluoride) with pure β crystals. *Nat. Commun.* **12**, 675 (2021).
17. Zhu, Z. et al. Electrostriction-enhanced giant piezoelectricity via relaxor-like secondary crystals in extended-chain ferroelectric polymers. *Matter* **4**, 3696–3709 (2021).
18. Han, Z., Liu, Y., Chen, X., Xu, W. & Wang, Q. Enhanced piezoelectricity in poly(vinylidene fluoride-co-trifluoroethylene-co-chlorotrifluoroethylene) random terpolymers with mixed ferroelectric phases. *Macromolecules* **55**, 2703–2713 (2022).
19. Gao, F. et al. Morphotropic phase boundary in polarized organic piezoelectric materials. *Phys. Rev. Lett.* **130**, 246801 (2023).
20. Hu, X., You, M., Yi, N., Zhang, X. & Xiang, Y. Enhanced piezoelectric coefficient of PVDF-TrFE films via in situ polarization. *Front. Energy Res.* **9**, 621540 (2021).
21. Wen, D. et al. Piezoelectric and magnetoelectric effects of flexible magnetoelectric heterostructure PVDF-TrFE/FeCoSiB. *Int. J. Mol. Sci.* **23**, 15992 (2022).
22. Messer, D. K. et al. Effects of flexoelectric and piezoelectric properties on the impact-driven ignition sensitivity of P(VDF-TrFE)/nAl films. *Combust. Flame* **242**, 112181 (2022).
23. Qin, B. et al. Ultrahigh piezoelectric coefficients achieved by tailoring the sequence and nano-domain structure of P(VDF-TrFE). *Adv. Mater.* **37**, 2502708 (2025).
24. Liu, Y. Q. et al. Morphotropic phase boundary in irradiated ferroelectric polymers. *Adv. Mater.* **37**, 2502099 (2025).
25. Liu, Y. et al. Insights into the morphotropic phase boundary in ferroelectric polymers from the molecular perspective. *J. Phys. Chem. C.* **123**, 8727–8730 (2019).
26. Chen, X. et al. Relaxor ferroelectric polymer exhibits ultrahigh electromechanical coupling at low electric field. *Science* **375**, 1418–1422 (2022).
27. Park, D.-S. et al. Induced giant piezoelectricity in centrosymmetric oxides. *Science* **375**, 653–657 (2022).
28. Ross, G. J., Watts, J. F., Hill, M. P. & Morrissey, P. Surface modification of poly(vinylidene fluoride) by alkaline treatment1. The degradation mechanism. *Polymer* **41**, 1685–1696 (2000).
29. Li, D. & Liao, M. Dehydrofluorination mechanism, structure and thermal stability of pure fluoroelastomer (poly(VDF-ter-HFP-ter-TFE) terpolymer) in alkaline environment. *J. Fluor. Chem.* **201**, 55–67 (2017).
30. Wang, H., Yan, B., Hussain, Z., Wang, W. & Chang, N. Chemically graft aminated GO onto dehydro-fluorinated PVDF for preparation of homogenous DF-PVDF/GO-NH_2 ultrafiltration membrane with high permeability and antifouling performance. *Surf. Interfaces* **33**, 102255 (2022).
31. Sharma, J., Totee, C., Kulshrestha, V. & Ameduri, B. Spectroscopic evidence and mechanistic insights on dehydrofluorination of PVDF in alkaline medium. *Eur. Polym. J.* **201**, 112580 (2023).
32. Tan, S., Li, J., Gao, G., Li, H. & Zhang, Z. Synthesis of fluoropolymer containing tunable unsaturation by a controlled dehydrochlorination of P(VDF-co-CTFE) and its curing for high performance rubber applications. *J. Mater. Chem.* **22**, 18496–18504 (2012).
33. Zhang, Z., Wang, X., Tan, S. & Wang, Q. Superior electrostrictive strain achieved under low electric fields in relaxor ferroelectric polymers. *J. Mater. Chem. A* **7**, 5201–5208 (2019).
34. Wang, X., Qiao, B., Tan, S., Zhu, W. & Zhang, Z. Tuning the ferroelectric phase transition of PVDF by uniaxially stretching crosslinked PVDF films with CF=CH bonds. *J. Mater. Chem. C.* **8**, 11426–11440 (2020).
35. Le Goupil, F. et al. Enhanced electrocaloric response of vinylidene fluoride–based polymers via one-step molecular engineering. *Adv. Funct. Mater.* **31**, 2007043 (2021).
36. Le Goupil, F. et al. Double-bond-induced morphotropic phase boundary leads to enhanced electrocaloric effect in VDF-based polymer flexible devices. *ACS Appl. Energy Mater.* **6**, 12172–12179 (2023).
37. Qian, X. et al. High-entropy polymer produces a giant electrocaloric effect at low fields. *Nature* **600**, 664–669 (2021).
38. Rui, G. et al. Dual-functional high-entropy polymer exhibiting giant cross-energy couplings at low fields. *Small Sci.* **5**, 2400624 (2025).
39. Resende, P. M., Isasa, J.-D., Hadziioannou, G. & Fleury, G. Deciphering TrFE fingerprints in P(VDF-TrFE) by Raman spectroscopy: defect quantification and morphotropic phase boundary. *Macromolecules* **56**, 9673–9684 (2023).
40. Liu, Y. et al. Chirality-induced relaxor properties in ferroelectric polymers. *Nat. Mater.* **19**, 1169–1174 (2020).
41. Taguet, A., Ameduri, B. & Boutevin, B. Crosslinking of vinylidene fluoride-containing fluoropolymers. *Adv. Polym. Sci.* **184**, 127–211 (2005).

42. Betz, N. et al. A FTIR study of PVDF irradiated by means of swift heavy ions. *Nucl. Instr. Methods Phys. Res. B* **151**, 89–96 (1999).
43. Chen, G. et al. Surface de-fluorination and bond modification of CFx by high-density hydrogen plasma processing. *ACS Appl. Energy Mater.* **4**, 8615–8620 (2021).
44. Girardot, M., Tahon, J.-F., Lyskawa, J. & Barrau, S. New insights on the crystal structure of P(VDF-co-TrFE) copolymer (55/45 mol%) and influence on the high piezoelectric response. *Polymer* **325**, 128317 (2025).
45. Nakhmanson, S. M., Nardelli, M. B. & Bernholc, J. Ab initio studies of polarization and piezoelectricity in vinylidene fluoride and BN-based polymers. *Phys. Rev. Lett.* **92**, 115504 (2004).
46. Liu, Y., Chen, X., Han, Z. B., Zhou, H. M. & Wang, Q. Defects in poly (vinylidene fluoride)-based ferroelectric polymers from a molecular perspective. *Appl. Phys. Rev.* **9**, 031306 (2022).
47. Huang, Y.-Z. et al. Giant piezoelectric coefficient of polyvinylidene fluoride with rationally engineered ultrafine domains achieved by rapid freezing processing. *Adv. Mater.* **37**, 2412344 (2025).
48. Deng, C. et al. Self -powered insole plantar pressure mapping system. *Adv. Funct. Mater.* **28**, 1801606 (2018).
49. Tian, G. et al. Rich lamellar crystal baklava-structured PZT/PVDF piezoelectric sensor toward individual table tennis training. *Nano Energy* **59**, 574–581 (2019).
50. Tian, G. et al. Ultrathin epidermal P(VDF-TrFE) piezoelectric film for wearable electronics. *ACS Appl. Electron. Mater.* **5**, 1730–1737 (2023).
51. Bhavanasi, V., Kumar, V., Parida, K., Wang, J. & Lee, P. S. Enhanced piezoelectric energy harvesting performance of flexible PVDF-TrFE bilayer films with graphene oxide. *ACS Appl. Mater. Interfaces* **8**, 521–529 (2016).
52. Wang, B. et al. Achievement of a giant piezoelectric coefficient and piezoelectric voltage coefficient through plastic molecular-based ferroelectric materials. *Matter* **5**, 1296–1304 (2022).
53. Jiang, H. et al. VDF-content-guided selection of piezoelectric P(VDF-TrFE) films in sensing and energy harvesting applications. *Energy Convers. Manag.* **211**, 112771 (2020).

Acknowledgements

This research was supported by the National Natural Science Foundation of China (Grant No. 12274152 and 92366302, Y.L.), the Guangdong Ba-sic and Applied Basic Research Foundation (2024A1515010483, Y.L.), and the initial financial support from HUST (Y.L.). This work is also supported by Guangdong Provincial Key Laboratory of Manufacturing Equipment Digitization (2023B1212060012). The authors would thank the Analytical and Testing Center of Huazhong University of Science and Technology for the technical assistance.

Author contributions

Y.L. conceived the idea, designed the research, and supervised the project. Z.Y. synthesized polymer films and collected XRD, FTIR and AFM. Z.K.F. and C.Y.L. performed swelling, NMR and DSC measurements. Z.Y. performed electrical, dielectric, and electromechanical measurements. Z.Y. fabricated the sensor devices. Y.L., Z.Y., and H.T. analyzed the data. Y.L. wrote the manuscript with feedback from all authors. All authors participated in the analysis and discussion.

Competing interests

The authors declare no competing interests.

Additional information

Supplementary information The online version contains supplementary material available at https://doi.org/10.1038/s41467-025-63849-6.

Correspondence and requests for materials should be addressed to Yang Liu.

Peer review information *Nature Communications* thanks Satoshi Horike, Hoi Ri Moon, Lothar Wondraczek and the other, anonymous, reviewer(s) for their contribution to the peer review of this work. A peer review file is available.